Meccanica (2006) 41:599–609
DOI 10.1007/s11012-006-9006-x

# Series solutions of unsteady MHD flows above a rotating disk

**Hang Xu · Shi-Jun Liao**

Received: 13 November 2004 / Accepted: 27 February 2006 / Published online: 11 October 2006


**Abstract** The series solutions of unsteady flows of a viscous incompressible electrically conducting fluid caused by an impulsively rotating infinite disk are given by means of an analytic technique, namely the homotopy analysis method. Using a set of new similarity transformations, we transfer the Navier–Stokes equations into a pair of nonlinear partial differential equations. The convergent series solutions are obtained, which are uniformly valid for all dimensionless time $0 \leq \tau < \infty$ in the whole spatial region $0 \leq \eta < \infty$. To the best of our knowledge, such kind of series solutions have never been reported. The effect of magnetic number on the velocity is investigated.

**Keywords** MHD flows · Unsteady · Von Kármán's flow · Homotopy analysis method · Mechanics of fluids

## 1 Introduction

The swirling flow due to an infinite rotating disk is a classic problem in fluid mechanics with numerous applications in science and engineering. Von Kármán [1] initiated the study of this problem. Using a set of similarity transformations, he reduced the full of Navier–Stokes equations to a pair of nonlinear ordinary differential equations in the axial coordinate. Cochran [2] corrected a few of errors in Von Kármán's approximations and obtained an accurate solution. Thiriot [3] made a start on the impulsively started initial-value rotating disk problem. However, his formulations contain numerical errors. Benton [4] extended the problem to the case of the flow started impulsively from rest and obtained a highly accurate solution by a simple analytical-numerical method. Then, the problem is generalized to include the case where the fluid itself is rotating as a solid body far from the disk with suction or injection at the disk surface. This introduces a parameter, i.e. the ratio of the angular velocity of the fluid at infinity to the angular velocity of the disk. Another generalization is to consider the viscous flow between two infinite coaxial rotating disks with suction or injection at both disks and this introduces another parameter, i.e. the Reynolds number determined by the distance of the two disks. All these problems are studied, theoretically, numerically and experimentally, by many researchers such as [5–18] and so on. For details, please refer to Zandbergen and Dijkstra [19].

The classical problem of the Von Kármán swirling viscous flow has been generalized in the manner to include diverse physical effects. Millsaps and Pohlhausen [20] first considered the

H. Xu · S.-J. Liao (✉)
School of Naval Architecture, Ocean and Civil Engineering, Shanghai JiaoTong University, Shanghai 200030, China
e-mail: sjliao@sjtu.edu.cn

steady-state heat transfer from a rotating disk maintained at a constant temperature for a variety of Prandtl numbers. Sparrow and Cess [21] and Loffredo [22] investigated the effect of the electrically conducting fluid characteristics on the flows caused by a rotating disk. Andersson and de Korte [23] studied the Magnetohydrodynamic flow of an electrically conducting power-law fluid due to an infinite rotating disk in the presence of an uniform magnetic field. Takhar et al. [24] investigated the unsteady MHD flows above an infinite rotating disk by assuming that the unsteadiness in the flow field is caused by the angular velocity of the disk which varies with time. Hayat et al. [25] studied the flows of a second order fluid due to noncoaxial rotations of a porous disk and a fluid at infinity in presence of a uniform transverse magnetic field.

In general, it is hard to analytically solve nonlinear problems. The widely applied perturbation techniques depend strongly upon small parameters and therefore are valid in general only for weakly nonlinear problems. In 1992, using the concept of homotopy [26], which is a basic concept of topology [27], Liao [28] proposed an analytic method for nonlinear problems, namely the homotopy analysis method (HAM), and modified it step by step [29–33]. Different from perturbation techniques, the HAM is independent upon small parameters at all, so that it is valid for highly nonlinear problems, especially those without small/large physical parameters. Besides, it logical contains the nonperturbation techniques such as Lyapunov's artificial small parameter method [34], Adomian decomposition method [35] and $\delta$-expansion method [36], as proved by Liao [37]. The so-called "homotopy perturbation method" [38] proposed in 1999 is only a special case of the HAM, as pointed out by Liao [39]. Thus, the HAM is more general and is a unification of previous nonperturbation techniques. Besides, different from all previous analytic methods, the HAM always gives us a family of series solutions whose convergence region can be adjusted and controlled by an auxiliary parameter. For details, please refer to Liao [37]. The HAM has been successfully applied to many types of nonlinear problems ([37, 40–47]), including some unsteady nonlinear problems [45–47]. Especially, new solutions of a few nonlinear problems are even found by means of it [48, 49]. All of these verify the validity of the HAM for highly nonlinear problems. The aim of the present paper is to investigate the unsteady flow of a viscous incompressible electrically conducting fluid (which is sometimes also called resistive fluid) caused by an impulsively rotating infinite disk by means of the HAM, and to obtain the convergent series solutions valid for all dimensionless time $0 \leq \tau < \infty$ in the whole spatial region $0 \leq \eta < \infty$. To the best of our knowledge, such kind of series solutions have never been reported.

## 2 Mathematical description

Let $(r, \phi, z)$ denote the coordinates in the radial, tangential and axial directions, $(u, v, w)$ the velocity components in these directions, and $t$ the time, respectively. Consider the unsteady, laminar flows of a viscous, incompressible electrically conducting fluid introduced by an infinite disk (at $z = 0$) which is started impulsively (at $t = 0$) into steady rotation with constant angular velocity $\Omega$ ($\Omega \neq 0$). The flow is governed by the continuity equation, the Navier–Stokes equations, and the generalized Ohm's law (without Hall effect), i.e.

$$\nabla \cdot \mathbf{V} = 0, \tag{1}$$

$$\frac{\partial \mathbf{V}}{\partial t} + (\mathbf{V} \cdot \nabla)\mathbf{V} = -\frac{1}{\rho}\nabla \mathbf{p} + \nu \nabla^2 \mathbf{V} + \frac{1}{\rho}(\mathbf{J} \times \mathbf{B}), \tag{2}$$

$$\mathbf{J} = \sigma[\mathbf{E} + \mathbf{V} \times \mathbf{B}], \tag{3}$$

where $\mathbf{p}$ is the pressure, $\mathbf{V}$ the fluid velocity, $\mathbf{J}$ the electric current density, $\mathbf{E}$ the electric field, $\mathbf{B}$ the total magnetic field, $\mathbf{B}_0$ the magnetic field in the $z$-direction, $\mathbf{b} = \mathbf{B} - \mathbf{B}_0$ the induced magnetic field, respectively. Assume that the flow is axisymmetric, and the magnetic Reynolds number is small, i.e. $Re_m = \mu_0 \sigma V L \ll 1$, where $\mu_0$ is the magnetic permeability, $\sigma$ the electrical conductivity, $V$ and $L$ the characteristic velocity and length, respectively. With these assumptions, it is reasonable to neglect the induced magnetic field $\mathbf{b}$ in comparison to the applied magnetic field $\mathbf{B}_0$. The electric field is defined by

$$\mathbf{E} = -\nabla \phi_E(r, z), \tag{4}$$

where $\phi_E(r, z) = Cr^2 + \Phi_E(z)$ is a general form of electric potential function of the similarity solutions,

$C$ is a constant, and $\Phi_E(z)$ is the electric potential function in the axial direction, respectively. In this article, $C$ is enforced to be zero. Otherwise, there would be a radial electric field far from the disk that the electric field must be externally imposed and does not arise from the rotating of the disk. Then there would be radial electric current, that would drive an azimuthal velocity. As a result, the problem becomes a completely different ones, i.e. the electromagnetically driven flow. Thus, we had to enforce $C = 0$ here. Note that the axial electric field caused by $\Phi_E(z)$ does not appear in the equations governing the flows. The reason is that the tangential velocity $v$ drives a radial electric current which varies linearly with $r$. Continuity of the current implied that there must be an axial electric current which is independent of $r$, but it does not produce any body force. Considering all of these, we have the governing equations of the unsteady boundary layer flows (refer to [21, 24, 50])

$$\frac{\partial u}{\partial r} + \frac{u}{r} + \frac{\partial w}{\partial z} = 0, \tag{5}$$

$$\frac{\partial u}{\partial t} + u\frac{\partial u}{\partial r} + w\frac{\partial u}{\partial z} - \frac{v^2}{r} = -\frac{1}{\rho}\frac{\partial p}{\partial r} - \frac{\sigma B^2 u}{\rho} + \nu\left(\nabla^2 u - \frac{u}{r^2}\right), \tag{6}$$

$$\frac{\partial v}{\partial t} + u\frac{\partial v}{\partial r} + w\frac{\partial v}{\partial z} + \frac{uv}{r} = -\frac{\sigma B^2 v}{\rho} + \nu\left(\nabla^2 v - \frac{v}{r^2}\right), \tag{7}$$

$$\frac{\partial w}{\partial t} + u\frac{\partial w}{\partial r} + w\frac{\partial w}{\partial z} = -\frac{1}{\rho}\frac{\partial p}{\partial z} + \nu\nabla^2 w, \tag{8}$$

subject to the initial and boundary conditions

$$\begin{aligned} &u = v = w = 0, \quad \text{at } t = 0,\\ &u = w = 0, \quad v = r\Omega, \quad \text{at } z = 0, \ t > 0,\\ &u = v = 0, \quad \text{as } z \to \infty, \ t \geq 0, \end{aligned} \tag{9}$$

where $p$ is the pressure, $\rho$ the density of the fluid, $\nu$ the kinematic viscosity of the fluid, $B$ the strength of applied magnetic field, respectively.

Following Williams and Rhyne [51], we use the following new similarity transformations

$$\begin{aligned} &\eta = z\sqrt{\frac{\Omega}{\nu\xi}}, \quad \xi = 1 - \exp(-\tau), \ \tau = \Omega t,\\ &u = r\Omega F, \ v = r\Omega G, \ w = (\Omega\nu\xi)^{1/2} H,\\ &p = -\rho\nu\Omega P, \end{aligned} \tag{10}$$

where $F$, $G$, $H$ and $P$ are real functions of $\eta$ and $\xi$. Then, Eqs. 5–8 become

$$H_\eta + 2F = 0, \tag{11}$$

$$(1-\xi)\left(\xi F_\xi - \frac{\eta}{2}F_\eta\right) - F_{\eta\eta} + \xi\left(HF_\eta + F^2 - G^2 + MF\right) = 0, \tag{12}$$

$$(1-\xi)\left(\xi G_\xi - \frac{\eta}{2}G_\eta\right) - G_{\eta\eta} + \xi\left(HG_\eta + 2FG + MG\right) = 0, \tag{13}$$

$$(1-\xi)\left(\frac{1}{2}H + \xi H_\xi - \frac{\eta}{2}H_\eta\right) + \xi HH_\eta - P_\eta - H_{\eta\eta} = 0, \tag{14}$$

subject to the boundary conditions

$$\begin{aligned} &F(0,\xi) = 0, \quad G(0,\xi) = 1, \quad H(0,\xi) = 0,\\ &F(\infty,\xi) = 0, \quad G(\infty,\xi) = 0, \end{aligned} \tag{15}$$

where $M = \sigma B^2/(\rho\Omega)$ is the magnetic number.

According to (14), it is easy to get $P$ for given $H$. From (11), it holds

$$F = -\frac{1}{2}H_\eta. \tag{16}$$

Substituting (16) into Eqs. 12 and 13, we obtain

$$(1-\xi)\left(\frac{\eta}{2}H_{\eta\eta} - \xi H_{\eta\xi}\right) + H_{\eta\eta\eta} + \xi\left(\frac{1}{2}H_\eta^2 - HH_{\eta\eta} - 2G^2 - MH_\eta\right) = 0, \tag{17}$$

$$(1-\xi)\left(\xi G_\xi - \frac{\eta}{2}G_\eta\right) - G_{\eta\eta} + \xi\left(HG_\eta - GH_\eta + MG\right) = 0, \tag{18}$$

subject to the boundary conditions

$$\begin{aligned} &G(0,\xi) = 1, \quad H(0,\xi) = H_\eta(0,\xi) = 0,\\ &G(\infty,\xi) = H_\eta(\infty,\xi) = 0. \end{aligned} \tag{19}$$

When $\xi = 0$, corresponding to $\tau = 0$, we have from (17) and (18) that

$$H_{\eta\eta\eta} + \frac{\eta}{2}H_{\eta\eta} = 0, \tag{20}$$

$$G_{\eta\eta} + \frac{\eta}{2}G_\eta = 0, \tag{21}$$

subject to the boundary conditions

$$\begin{aligned} &G(0,0) = 1, \ H(0,0) = H_\eta(0,0) = 0,\\ &G(\infty,0) = H_\eta(\infty,0) = 0. \end{aligned} \tag{22}$$

The above equations have the exact solutions

$$H(\eta,0) = 0, \quad G(\eta,0) = \operatorname{erfc}\left(\frac{\eta}{2}\right), \tag{23}$$

where erfc $(\eta)$ is the error function defined by

$$\operatorname{erfc}(\eta) = \frac{2}{\sqrt{\pi}} \int_{\eta}^{+\infty} \exp(-z^2)\mathrm{d}z. \tag{24}$$

When $\xi = 1$, corresponding to $\tau \to +\infty$, we have

$$H_{\eta\eta\eta} + \frac{1}{2}H_{\eta}^2 - HH_{\eta\eta} - 2G^2 - MH_{\eta} = 0, \tag{25}$$

$$G_{\eta\eta} - HG_{\eta} + GH_{\eta} - MG = 0, \tag{26}$$

subject to the boundary conditions

$$G(0,1) = 1, \quad H(0,1) = H_{\eta}(0,1) = 0,$$
$$G(\infty,1) = H_{\eta}(\infty,1) = 0. \tag{27}$$

The skin friction coefficients in radial and tangential directions are given by

$$C_f^r = \frac{\tau_r}{\rho(r\Omega)^2} = -\frac{1}{\sqrt{\xi Re_r}} F_{\eta}(0,\xi) = \frac{1}{2\sqrt{\xi Re_r}} H_{\eta\eta}(0,\xi), \tag{28}$$

$$C_f^{\phi} = \frac{\tau_{\phi}}{\rho(r\Omega)^2} = -\frac{1}{\sqrt{\xi Re_r}} G_{\eta}(0,\xi), \tag{29}$$

where $Re_r = r\sqrt{\Omega/\nu}$ is the local Reynolds number, $\tau_r$ and $\tau_{\phi}$ are the radial and tangential shear stress, respectively.

## 3 Homotopy analysis solution

Liao [37] studied the steady-state Von kármán swirling viscous flow by means of the HAM. Following Liao [37], we introduce the transformation

$$\eta = \lambda\zeta, \tag{30}$$

where $\lambda > 0$ is the so-called spatial-scale parameter. Using (30), Eqs. 17 and 18 become

$$(1-\xi)\left(\frac{\zeta}{2\lambda}H_{\zeta\zeta} - \frac{\xi}{\lambda}H_{\zeta\xi}\right) + \frac{1}{\lambda^3}H_{\zeta\zeta\zeta} + \xi\left[\frac{1}{2\lambda^2}H_{\zeta}^2 - \frac{1}{\lambda^2}HH_{\zeta\zeta} - 2G^2 - \frac{M}{\lambda}H_{\zeta}\right] = 0, \tag{31}$$

$$(1-\xi)\left(\xi G_{\xi} - \frac{\zeta}{2}G_{\zeta}\right) - \frac{1}{\lambda^2}G_{\zeta\zeta} + \xi\left(\frac{1}{\lambda}HG_{\zeta} - \frac{1}{\lambda}GH_{\zeta} + MG\right) = 0, \tag{32}$$

subject to the boundary conditions

$$G(0,\xi) = 1, \quad H(0,\xi) = H_{\zeta}(0,\xi) = 0,$$
$$G(\infty,\xi) = H_{\zeta}(\infty,\xi) = 0. \tag{33}$$

From the boundary conditions (33), it is obvious that $G(\zeta,\xi)$ and $H(\zeta,\xi)$ can be expressed by a set of base functions

$$\left\{\xi^k\ \zeta^m\ \exp(-n\zeta)|\ k \geq 0,\ n \geq 0,\ m \geq 0\right\} \tag{34}$$

in the form

$$H(\zeta,\xi) = \sum_{k=0}^{+\infty}\sum_{m=0}^{+\infty}\sum_{n=0}^{+\infty} a_{m,n}^k \xi^k \zeta^m \exp(-n\zeta), \tag{35}$$

$$G(\zeta,\xi) = \sum_{k=0}^{+\infty}\sum_{m=0}^{+\infty}\sum_{n=0}^{+\infty} b_{m,n}^k \xi^k \zeta^m \exp(-n\zeta), \tag{36}$$

where $a_{m,n}^k$ and $b_{m,n}^k$ are coefficients. These provide us with the *solution expressions* of $H(\zeta,\xi)$ and $G(\zeta,\xi)$, respectively. From (33), (35) and (36), it is straightforward to choose

$$H_0(\zeta,\xi) = 0, \quad G_0(\zeta,\xi) = \exp(-\zeta), \tag{37}$$

as the initial approximations of $H(\zeta,\xi)$ and $G(\zeta,\xi)$. Similarly, it is natural to choose

$$\mathcal{L}_H[\Phi(\xi,\zeta;q)] = \frac{\partial^3\Phi}{\partial\zeta^3} - \frac{\partial\Phi}{\partial\zeta},$$
$$\mathcal{L}_G[\Psi(\xi,\zeta;q)] = \frac{\partial^2\Psi}{\partial\zeta^2} - \Psi, \tag{38}$$

as the auxiliary linear operators. They have the following properties

$$\mathcal{L}_H[C_1\exp(-\zeta) + C_2\exp(\zeta) + C_3] = 0, \tag{39}$$

$$\mathcal{L}_G[C_4\exp(-\zeta) + C_5\exp(\zeta)] = 0, \tag{40}$$

where $C_1$, $C_2$, $C_3$, $C_4$, and $C_5$ are constants. Based on Eqs. 31 and 32, we define the nonlinear operators

$$\mathcal{N}_H[\Phi(\zeta,\xi;q),\Psi(\zeta,\xi;q)] = (1-\xi)\left(\frac{\zeta}{2\lambda}\frac{\partial^2\Phi}{\partial\zeta^2} - \frac{\xi}{\lambda}\frac{\partial^2\Phi}{\partial\xi\partial\zeta}\right) + \frac{1}{\lambda^3}\frac{\partial^3\Phi}{\partial\zeta^3} + \xi\left[\frac{1}{2\lambda^2}\left(\frac{\partial\Phi}{\partial\zeta}\right)^2 - \frac{1}{\lambda^2}\Phi\frac{\partial^2\Phi}{\partial\zeta^2} - 2\Psi^2 - \frac{M}{\lambda}\frac{\partial\Phi}{\partial\zeta}\right], \tag{41}$$

$$\mathcal{N}_G[\Phi(\zeta,\xi;q),\Psi(\zeta,\xi;q)] = (1-\xi)\left(\xi\frac{\partial\Psi}{\partial\xi} - \frac{\zeta}{2}\frac{\partial\Psi}{\partial\zeta}\right) - \frac{1}{\lambda^2}\frac{\partial^2\Psi}{\partial\zeta^2} + \xi\left(\frac{1}{\lambda}\Phi\frac{\partial\Psi}{\partial\zeta} - \frac{1}{\lambda}\Psi\frac{\partial\Phi}{\partial\zeta} + M\Psi\right). \tag{42}$$

Then, let $\hbar_H$ and $\hbar_G$ denote the nonzero auxiliary parameters. We construct the zeroth-order deformation equations

$$(1-q)\mathcal{L}_H[\Phi(\zeta,\xi;q)-H_0(\zeta,\xi)] = q\,\hbar_H\,\mathcal{N}_H[\Phi(\zeta,\xi;q),\Psi(\zeta,\xi;q)], \tag{43a}$$

$$(1-q)\mathcal{L}_G[\Psi(\zeta,\xi;q)-G_0(\zeta,\xi)] = q\,\hbar_G\,\mathcal{N}_G[\Phi(\zeta,\xi;q),\Psi(\zeta,\xi;q)], \tag{43b}$$

subject to the boundary conditions

$$\Psi(0,\xi;q)=1,\quad \Phi(0,\xi;q)=\left.\frac{\partial\Phi(\zeta,\xi;q)}{\partial\zeta}\right|_{\zeta=0} = \left.\frac{\partial\Phi(\zeta,\xi;q)}{\partial\zeta}\right|_{\zeta=+\infty}=\Psi(\infty,\xi;q)=0, \tag{44}$$

where $q\in[0,1]$ is an embedding parameter. Obviously, when $q=0$ and $q=1$, the zeroth-order deformation equations (43a) to (43b) have the solutions

$$\Phi(\zeta,\xi;0)=H_0(\zeta,\xi),\quad \Psi(\zeta,\xi;0)=G_0(\zeta,\xi), \tag{45}$$

and

$$\Phi(\zeta,\xi;1)=H(\zeta,\xi),\quad \Psi(\zeta,\xi;1)=G(\zeta,\xi), \tag{46}$$

respectively. Expending $\Phi(\zeta,\xi;q)$ and $\Psi(\zeta,\xi;q)$ in Taylor's series with respect to $q$, we have

$$\Phi(\zeta,\xi;q)=H_0(\zeta,\xi)+\sum_{m=1}^{+\infty}H_m(\zeta,\xi)\,q^m, \tag{47}$$

$$\Psi(\zeta,\xi;q)=G_0(\zeta,\xi)+\sum_{m=1}^{+\infty}G_m(\zeta,\xi)\,q^m, \tag{48}$$

where

$$H_m(\zeta,\xi)=\left.\frac{1}{m!}\frac{\partial^m\Phi(\zeta,\xi;q)}{\partial q^m}\right|_{q=0},\quad G_m(\zeta,\xi)=\left.\frac{1}{m!}\frac{\partial^m\Psi(\zeta,\xi;q)}{\partial q^m}\right|_{q=0}. \tag{49}$$

Note that Eqs. (43a) and (43b) contain two auxiliary parameters $\hbar_H$ and $\hbar_G$. Assuming that all of them are properly chosen so that the above series are convergent at $q=1$, we have, using (45), the solution series

$$H(\zeta,\xi)=H_0(\zeta,\xi)+\sum_{m=1}^{+\infty}H_m(\zeta,\xi), \tag{50}$$

$$G(\zeta,\xi)=G_0(\zeta,\xi)+\sum_{m=1}^{+\infty}G_m(\zeta,\xi). \tag{51}$$

For the sake of simplicity, define vectors

$$\vec{H}_m=\{H_0,H_1,H_2,\ldots,H_m\},\quad \vec{G}_m=\{G_0,G_1,G_2,\ldots,G_m\}. \tag{52}$$

Differentiating the zeroth-order deformation equations (43a) and (43b) $m$ times with respect to $q$, then setting $q=0$, and finally dividing them by $m!$, we obtain the $m$th-order deformation equations

$$\mathcal{L}_H[H_m(\zeta,\xi)-\chi_m H_{m-1}(\zeta,\xi)] = \hbar_H R_m^H(\vec{H}_{m-1},\vec{G}_{m-1}), \tag{53a}$$

$$\mathcal{L}_G[G_m(\zeta,\xi)-\chi_m G_{m-1}(\zeta,\xi)] = \hbar_G R_m^G(\vec{H}_{m-1},\vec{G}_{m-1}), \tag{53b}$$

subject to the boundary conditions

$$H_m(0,\xi)=G_m(0,\xi)=\left.\frac{\partial H_m(\zeta,\xi)}{\partial\zeta}\right|_{\zeta=0}=0,\quad G_m(\infty,\xi)=\left.\frac{\partial H_m(\zeta,\xi)}{\partial\zeta}\right|_{\zeta=\infty}=0, \tag{54}$$

where

$$\begin{aligned}R_m^H(\vec{H}_{m-1},\vec{G}_{m-1}) &= (1-\xi)\times\left(\frac{\zeta}{2\lambda}\frac{\partial^2H_{m-1}}{\partial\zeta^2}-\frac{\xi}{\lambda}\frac{\partial^2H_{m-1}}{\partial\xi\partial\zeta}\right)+\frac{1}{\lambda^3}\frac{\partial^3H_{m-1}}{\partial\zeta^3}+\xi\left[\sum_{n=0}^{m-1}\left(\frac{1}{2\lambda^2}\frac{\partial H_n}{\partial\zeta}\frac{\partial H_{m-1-n}}{\partial\zeta}\right.\right.\\ &\quad -\frac{1}{\lambda^2}H_n\frac{\partial^2H_{m-1-n}}{\partial\zeta^2}\\ &\quad \left.\left.-2G_nG_{m-1-n}\right)-\frac{M}{\lambda}\frac{\partial H_{m-1}}{\partial\zeta}\right],\end{aligned} \tag{55}$$

$$\begin{aligned}R_m^G(\vec{H}_{m-1},\vec{G}_{m-1}) &= (1-\xi)\times\left(\xi\frac{\partial G_{m-1}}{\partial\xi}-\frac{\zeta}{2}\frac{\partial G_{m-1}}{\partial\zeta}\right)-\frac{1}{\lambda^2}\frac{\partial^2G_{m-1}}{\partial\zeta^2}\\ &\quad +\xi\left[\sum_{n=0}^{m-1}\left(\frac{1}{\lambda}H_n\frac{\partial G_{m-1-n}}{\partial\zeta}-\frac{1}{\lambda}G_n\frac{\partial H_{m-1-n}}{\partial\zeta}\right)\right.\\ &\quad \left.+MG_{m-1}\right],\end{aligned} \tag{56}$$

and

$$\chi_m=\begin{cases}0, m=1,\\ 1, m>1.\end{cases} \tag{57}$$

Note that, substituting (47) and (48) into zeroth-order deformation equations (43a)–(44), and equating the same power of $q$, one can obtain exactly the same high-order deformation equations as Eqs. (53a)–(57).

Let $H_m^*(\zeta,\xi)$ and $G_m^*(\zeta,\xi)$ denote the particular solutions of Eqs. 53a and 53b. According to (39) and (40), the general solutions read

$$H_m(\zeta,\xi) = H_m^*(\zeta,\xi) + C_1\exp(-\zeta) + C_2\exp(\zeta) + C_3, \tag{58}$$

$$G_m(\zeta,\xi) = G_m^*(\zeta,\xi) + C_4\exp(-\zeta) + C_5\exp(\zeta), \tag{59}$$

where the integral coefficients $C_1$, $C_2$, $C_3$, $C_4$, and $C_5$ are determined by the boundary condition (54), i.e.

$$C_1(\xi) = \left.\frac{\partial H_m^*}{\partial\eta}\right|_{\eta=0}, \quad C_3(\xi) = -C_1 - H_m^*(0,\xi),$$
$$C_4(\xi) = -G_m^*(0,\xi), \quad C_2(\xi) = C_5(\xi) = 0. \tag{60}$$

In this way, it is easy to solve the set of the linear equations (53a), (53b) and (54) one after the other in the order $m = 1, 2, 3, \ldots$

## 4 Result analysis

Liao [37] proved that, as long as a solution series given by the HAM converges, it must be one of solutions. Note that the solution series (50) and (51) contain three auxiliary parameters: the spatial-scale parameter $\lambda$ and two auxiliary parameters $\hbar_H$ and $\hbar_G$. These auxiliary parameters can be determined in the following way. Note that the residual error of the initial guess $H_0(\xi,\zeta)$, i.e.

$$E_0(\lambda) = \int_0^1\int_0^\infty (R_1^H[\vec{H}_0,\vec{G}_0])^2 \mathrm{d}\xi\,\mathrm{d}\zeta, \tag{61}$$

is dependent only on $\lambda$. Enforcing

$$\frac{\mathrm{d}E_0}{\mathrm{d}\lambda} = 0, \tag{62}$$

we obtain the best value of $\lambda$ by solving the above equation. Thereafter, we can properly choose the values of $\hbar_H$ and $\hbar_G$ to ensure that the solution series (50) and (51) converge. This can be done by plotting the related $\hbar$-curves, as suggested by Liao [37].

When $\xi = 0$, corresponding to the initial state, our analytic approximations agree well with the exact solutions by means of $\hbar_H = -1/8$, $\hbar_G = -1/5$ and $\lambda = 1/2$, as shown in Fig. 1. When $\xi = 1$, corresponding to the steady state, our analytic approximations (given also by means of $\hbar_H = -1/8$, $\hbar_G = -1/5$ and $\lambda = 1/2$) agree well with numerical ones, as shown in Figs. 2–4. Furthermore, it is found that, in the *whole* region $\xi \in [0,1]$, the solution series (50) and (51) are convergent by means of $\hbar_H = -1/8$, $\hbar_G = -1/5$ and $\lambda = 1/2$, as shown in Figs. 5 and 6. Note that, the numerical results are given by the standard Keller–Box method [52]. Thus, by means of HAM, we obtain the convergent series solutions uniformly valid for *all* dimensionless time $0 \le \tau < +\infty$ in the *whole* spatial region $0 \le \eta < +\infty$.

As shown in Figs. 2–4, as $\tau \to \infty$ (corresponding to the steady-state flows), the velocity profiles of $F(\eta,\xi)$, $G(\eta,\xi)$ and $H(\eta,\xi)$ given by a lager $M$ are closer to their initial ones. The velocity profiles of $F(\eta,\xi)$, $G(\eta,\xi)$ and $H(\eta,\xi)$ for a given value of $M$ at different dimensionless time $\tau$ are plotted in Figs. 7–9, respectively. From these figures, it is clear how the velocities in three directions vary smoothly from the initial profile to the steady ones. Obviously, the effect of $M$ increases as $\xi$ increases.

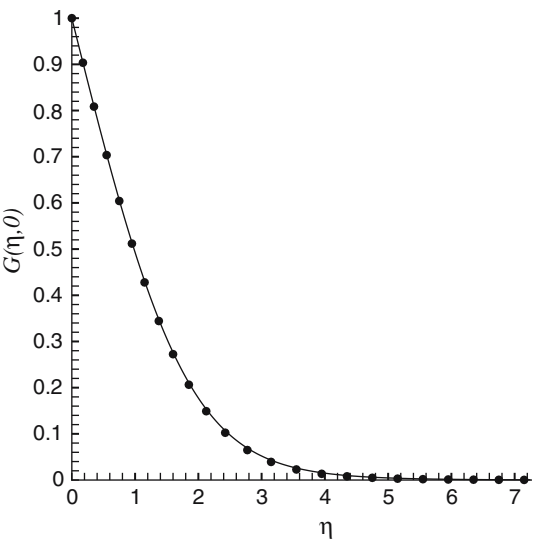


**Fig. 1** The comparison of $G(\eta,0)$ of the exact solution with the series solution given by HAM. Symbol: exact solution; Solid line: 20th order HAM approximations

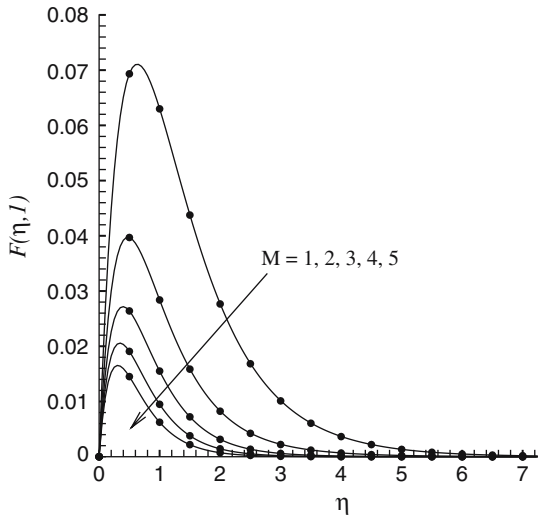


**Fig. 2** The comparison of $F(\eta,1)$ of the numerical results with the series solutions given by HAM. Symbol: numerical results; Solid line: 20th order HAM approximations

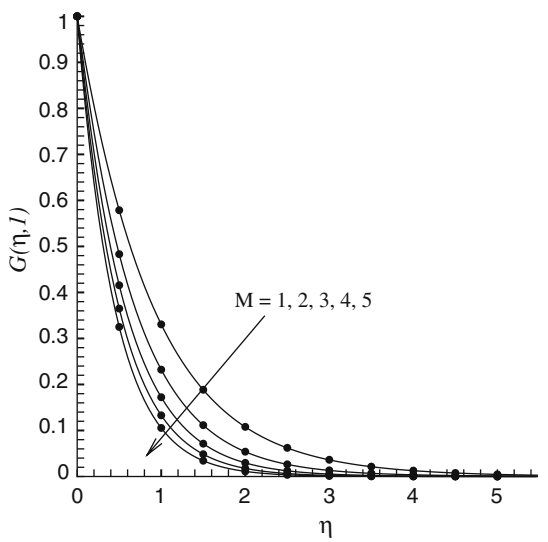


**Fig. 3** The comparison of $G(\eta,1)$ of the numerical results with the series solutions given by HAM. Symbol: numerical results; Solid line: 20th order HAM approximations

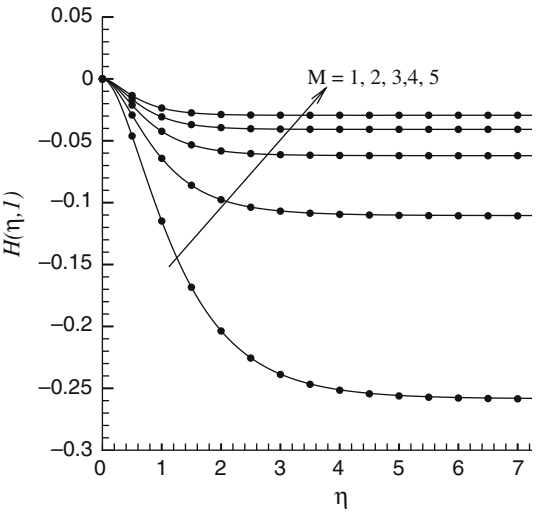


**Fig. 4** The comparison of $H(\eta,1)$ of the numerical results with the series solutions given by HAM. Symbol: numerical results; Solid line: 20th order HAM approximations

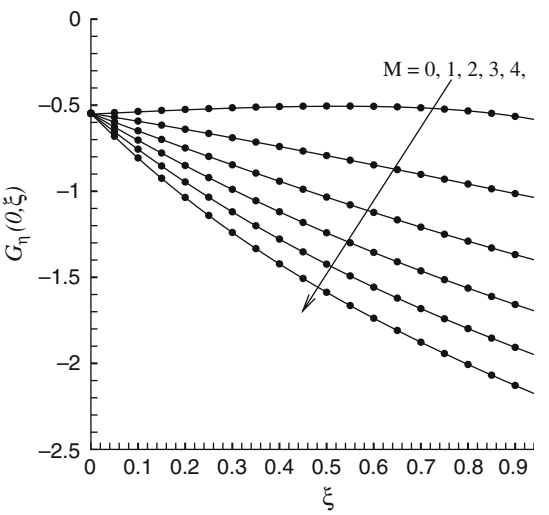


**Fig. 5** The approximations of $G_\eta(0,\xi)$ for $0 \le \xi \le 1$ given by HAM. Symbol: numerical results; Solid line: 20th order HAM approximations

At the 10th-order approximation, we have

$$
\begin{aligned}
G_\eta(0,\xi) = {} & -0.601101 + 0.132151\xi \\
& - 0.528604M\xi - 0.0331501\xi^2 - 0.11527M\xi^2 \\
& + 0.0768466M^2\xi^2 - 0.0235569\xi^3 \\
& - 0.0127696M\xi^3 + 0.0497901M^2\xi^3 \\
& - 0.0132774M^3\xi^3 - 0.0127191\xi^4 \\
& + 8.02033\times 10^{-3}M\xi^4 + 0.0188366M^2\xi^4 \\
& - 0.0200754M^3\xi^4 + 3.09269\times 10^{-3}M^4\xi^4 \\
& - 0.0127425\xi^5 + 0.0332359M\xi^5 - 0.0144771M^2\xi^5 \\
& - 7.60698\times 10^{-3}M^3\xi^5 + 4.62141\times 10^{-3}M^4\xi^5 \\
& - 4.3974\times 10^{-4}M^5\xi^5 - 6.36733\times 10^{-3}\xi^6 \\
& + 0.0217058M\xi^6 - 0.0190299M^2\xi^6 \\
& + 2.7585\times 10^{-3}M^3\xi^6 + 2.52421\times 10^{-3}M^4\xi^6
\end{aligned}
$$

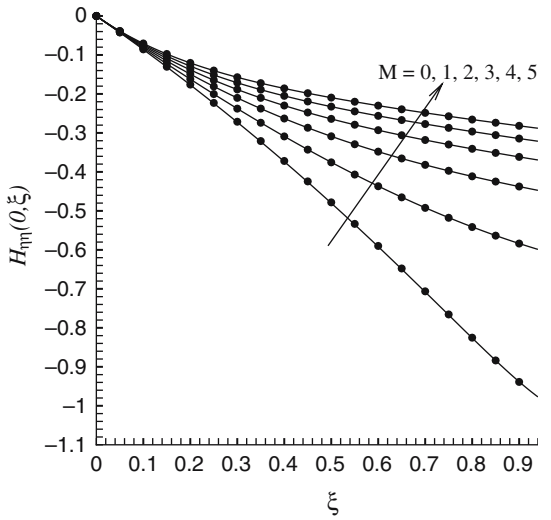


**Fig. 6** The approximations of $H_{\eta\eta}(0,\xi)$ for $0 \le \xi \le 1$ given by HAM. Symbol: numerical results; Solid line: 20th order HAM approximations

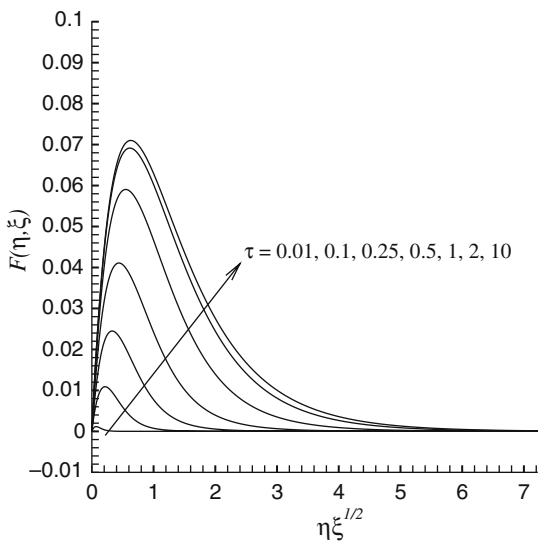


**Fig. 7** The velocity profile of $F(\eta,\xi)$ at different dimensionless time $\tau = \Omega t$ when $M = 1$

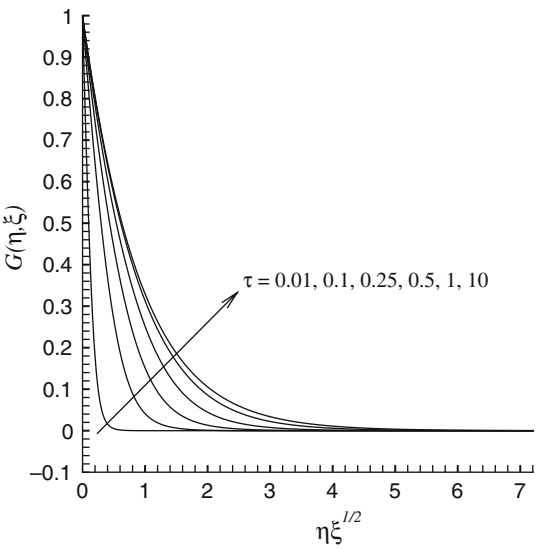


**Fig. 8** The velocity profile of $G(\eta,\xi)$ at different dimensionless time $\tau = \Omega t$ when $M = 1$

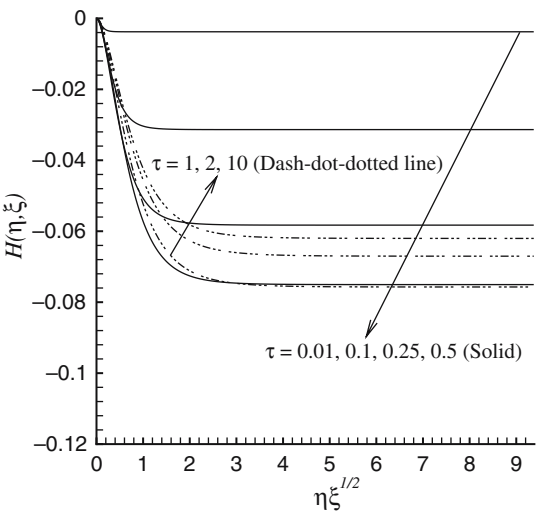


**Fig. 9** The velocity profile of $H(\eta,\xi)$ at different dimensionless time $\tau = \Omega t$ when $M = 3$

$$
\begin{aligned}
&- 8.27673 \times 10^{-4} M^5 \xi^6 + 5.33717 \times 10^{-5} M^6 \xi^6 \\
&- 3.24591 \times 10^{-3} \xi^7 + 0.0129431 M \xi^7 \\
&- 0.0152168 M^2 \xi^7 + 6.4807 \times 10^{-3} M^3 \xi^7 \\
&- 1.33489 \times 10^{-4} M^4 \xi^7 - 5.75257 M^5 \times 10^{-4} \xi^7 \\
&+ 1.19854 \times 10^{-4} M^6 \xi^7 - 5.57692 \times 10^{-6} M^7 \xi^7 \\
&- 1.77707 \times 10^{-3} \xi^8 + 7.61521 \times 10^{-3} M \xi^8 \\
&- 0.0102117 M^2 \xi^8 + 5.89746 \times 10^{-3} M^3 \xi^8 \\
&- 1.27811 \times 10^{-3} M^4 \xi^8 - 1.42947 \times 10^{-4} M^5 \xi^8 \\
&+ 1.09198 \times 10^{-4} M^6 \xi^8 - 1.51388 \times 10^{-5} M^7 \xi^8 \\
&+ 5.32289 \times 10^{-7} M^8 \xi^8 - 5.6943 \times 10^{-4} \xi^9 \\
&+ 3.36237 \times 10^{-3} M \xi^9 - 5.85884 \times 10^{-3} M^2 \xi^9 \\
&+ 4.74345 \times 10^{-3} M^3 \xi^9 - 1.99918 \times 10^{-3} M^4 \xi^9 \\
&+ 4.11681 \times 10^{-4} M^5 \xi^9 - 1.990213 \times 10^{-5} M^6 \xi^9 \\
&- 6.28583 \times 10^{-6} M^7 \xi^9 + 8.82624 \times 10^{-7} M^8 \xi^9 \\
&- 2.40856 \times 10^{-8} M^9 \xi^9 - 1.24696 \times 10^{-3} \xi^{10} \\
&+ 4.59667 \times 10^{-3} M \xi^{10} - 5.42665 \times 10^{-3} M^2 \xi^{10}
\end{aligned}
$$

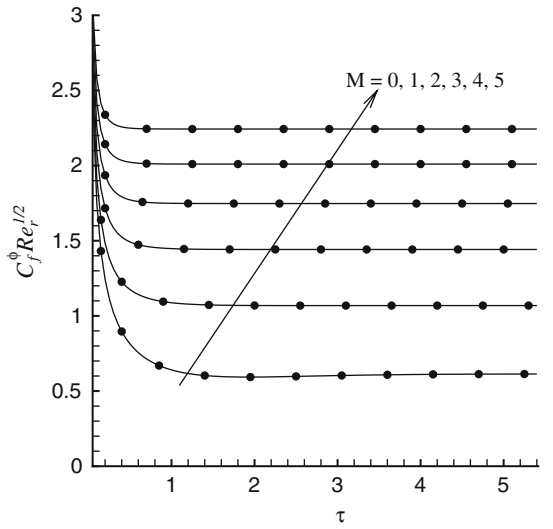


**Fig. 10** The comparison of $C_f^{\phi}\sqrt{Re_r}$ versus $\tau = \Omega t$ at different values of $M$. Symbol: Numerical results; Solid line: 10th order HAM approximations

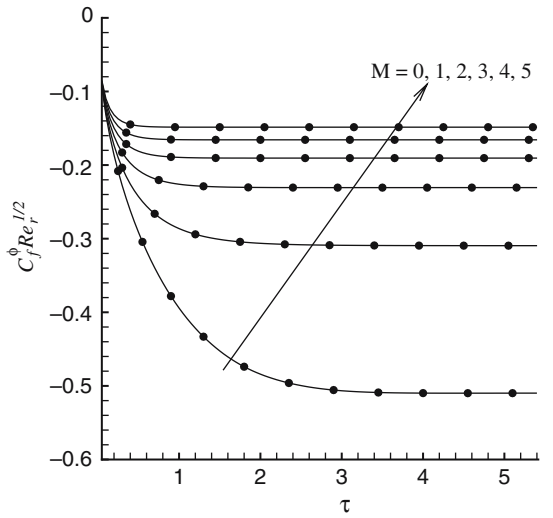


**Fig. 11** The comparison of $C_f^{r}\sqrt{Re_r}$ versus $\tau = \Omega t$ at different values of $M$. Symbol: Numerical results; Solid line: 10th order HAM approximations

$$
\begin{aligned}
&+2.54392\times10^{-3}M^3\xi^{10}-1.06227\times10^{-4}M^4\xi^{10}\\
&-3.94209\times10^{-4}M^5\xi^{10}+1.84336\times10^{-4}M^6\xi^{10}\\
&-4.06054\times10^{-5}M^7\xi^{10}+4.84525\times10^{-6}M^8\xi^{10}\\
&-2.91135\times10^{-7}M^9\xi^{10}+6.43814\times10^{-9}M^{10}\xi^{10}
\end{aligned}
\tag{63}
$$

and

$$
\begin{aligned}
H_{\eta\eta}(0,\xi) &= -0.753217\xi-0.157676\xi^2\\
&+0.250509M\xi^2-0.0464415\xi^3+0.154215M\xi^3\\
&-0.0742715M^2\xi^3-0.0172299\xi^4\\
&+0.0805866M\xi^4-0.0744303M^2\xi^4\\
&+0.0172259M^3\xi^4-0.00835926\xi^5\\
&+0.0436562M\xi^5-0.053977M^2\xi^5\\
&+0.0235009M^3\xi^5-0.00319522M^4\xi^5\\
&-0.00508063\xi^6+0.02603M\xi^6-0.0334615M^2\xi^6\\
&+0.0330929M^3\xi^6-0.0111802M^4\xi^6\\
&+0.00116494M^5\xi^6+0.00507428\xi^7\\
&-0.00447143M\xi^7-0.0117372M^2\xi^7\\
&+0.0189165M^3\xi^7-0.0100844M^4\xi^7\\
&+0.0022273M^5\xi^7-1.65816\times10^{-4}M^6\xi^7\\
&+0.00311045\xi^8-0.00488687M\xi^8\\
&-0.00253812M^2\xi^8+0.00885629M^3\xi^8\\
&-0.00657614M^4\xi^8+0.00220921M^5\xi^8\\
&-0.000343223M^6\xi^8+1.91458\times10^{-5}M^7\xi^8\\
&+0.0017117\xi^9-0.00348411M\xi^9\\
&+0.0004694M^2\xi^9\\
&+0.00344048M^3\xi^9-3.42764\times10^{-3}M^4\xi^9\\
&+1.50879\times10^{-3}M^5\xi^9-3.47059\times10^{-4}M^6\xi^9\\
&+3.96989\times10^{-5}M^7\xi^9-1.71444\times10^{-6}M^8\xi^9\\
&+1.11614\times10^{-3}\xi^{10}-2.68223\times10^{-3}M\xi^{10}\\
&+0.00118369M^2\xi^{10}+1.54803\times10^{-3}M^3\xi^{10}\\
&-2.03301\times10^{-3}M^4\xi^{10}+1.03751\times10^{-3}M^5\xi^{10}\\
&-2.88218\times10^{-4}M^6\xi^{10}+4.55016\times10^{-5}M^7\xi^{10}\\
&-3.78643\times10^{-6}M^8\xi^{10}+1.25618\times10^{-7}M^9\xi^{10}.
\end{aligned}
\tag{64}
$$

Substituting them into (28) and (29), we obtain the analytic expressions of $C_f^{\phi}$ and $C_f^{r}$. They agree well with the numerical results, as shown in Figs. 10 and 11. So, the 10th-order approximations of $C_f^{\phi}$ and $C_f^{r}$ are accurate enough, and are useful in applications. Note that, the skin friction stresses decreases as the value of $M$ increases. Physically speaking, the skin friction forces decreases when the magnetic field becomes stronger.

## 5 Conclusions

In this paper, we apply the HAM to obtain the series solutions of the unsteady flows of a viscous

incompressible electrically conducting fluid caused by an impulsively rotating infinite disk. Different from previous analytic solutions, our solutions are accurate and valid for *all* time $0 \leq \tau < \infty$ in the *whole* spatial space $0 \leq \eta < \infty$. The explicit analytic expressions of the surface skin friction coefficients at the 10th-order of approximation are given, which are accurate and valid for all time. To the best of our knowledge, such kind of solutions have never been reported. The effect of the electrically conducting fluid characteristics is also investigated. The proposed analytic approach has general meaning and thus can be applied in the similar way to other complicated unsteady boundary-layer flows so as to obtain accurate series solutions valid for all time.

The HAM has been successfully applied to find multiple solutions of some relatively simple equations, as shown in [37, 43, 48, 49]. When multiple steady-state solutions exist, it is very valuable to study the corresponding unsteady solutions and their stability. Notice that the equations of the viscous flows due to a rotating disk have multiple solutions, as pointed out by many researchers. However, it is still a challenge for us to find the multiple solution of the problem in this article, which is more complicated than those studied in [37, 38, 48, 49]. Further investigation will be done in this direction.

**Acknowledgements** Thanks to anonymous reviewers for their valuable comments and suggestions, which greatly improve this article. This work is partly sponsored by Program of Shanghai Subject Chief Scientist (Approval No. 05XD14011) and Shanghai Committee of Science and Technology (Approval No. 05DJ14001).

## References

1. Von Kármán T (1921) Über läminare und turbulence Reibung. Z Angew Math Mech 1:233–252
2. Cochran WG (1934) The flow due to a rotating disk. Proc Camb Phil Soc 30:365–375
3. Thiriot HK (1940) Über die laminare Anlaufströmung einer Flüssigkeit einem rotierenden Boden bei plötzlicher Änderung des drehungszustandes. Z Angew Math Mech 20:1–13
4. Benton ER (1966) On the flow due to a rotating disk. J Fluid Mech 24:781–800
5. Fettis HE (1955) On the integration of a class of differential equations occurring in boundary layer and other hydrodynamic problems. In: Proc 4th Midwestern Conf on Fluid Mech Purdue
6. Lance GN, Rogers MH (1962) The axial symmetric flow of a viscous fluid between two infinite rotating disks. Proc Roy Soc London Ser A 266:109–121
7. Mellor GL, Chapple PJ, Stokes VK (1968) On the flow between a roating and a stationary disk. J Fluid Mech 31:95–112
8. Tam KK (1969) A note on the asymptotic solution of the flow between two oppositely rotating infinite plane disks. SIAM J Appl Math 17:1305–1310
9. Schlichting H (1974) Boundary layer theory, 7th edn. McGraw-Hill, New York
10. Bodonyi RJ (1975) On the rotationlly symmetric flow above an infinite ratating disk. J Fluid Mech 67:657–666
11. Zandbergen PJ, Dijkstra D (1977) Non-unique solutions of the Navier–Stokes equations for the Kármán swirling flow. J Eng Math 11:167–188
12. Dijkstra D (1980) On the relation between adjacent invisid cell type solutions to the rotating-disk equations. J Eng Math 14:133–154
13. Holoniok M, Kubicek M, Hlavacek V (1981) Computation of the flow between two rotating coaxial disks: multiplicity of steady-state solutions. J Fluid Mech 81:227–240
14. Dijkstra D, Van Heijst GJF (1983) The flow between two finite rotating disks enclosed by a cylinder. J Fluid Mech 128:123–154
15. Szeri AZ, Schneider SJ, Labbe F, Kaufman HN (1983) Flow between rotating disks, part I: basic flow. J Fluid Mech 134:103–131
16. Bodonyi RJ, Ng BS (1984) On the stability of the similarity solutions for swirling flow above an infinite rotating disk. J Fluid Mech 144:311–328
17. Yang C, Liao Sj (2006) On the explicit, purely analytic solution of Von Krmn swirling viscous flow. Commun Nonlinear Sci Num Simulat 11:83–93
18. Volkan Ersoy H (2003) Unsteady flow due to concentric rotation of eccentric rotating disks. Meccanica 38:325–334
19. Zandbergen PJ, Dijkstra D (1987) Kármán swirling flows. Ann Rev Fluid Mech 19:465–491
20. Millspas K, Pohlhausen K (1952) Heat transfer by laminar flow from a rotating disk. J Aeronaut Sci 19:120–136
21. Sparrow EM, Cess RD (1962) Magnetohydrodynamic flow and heat transfer about a rotating disk. ASME J Appl Mech 29:181–187
22. Loffredo MI (1986) Extension of vón Kàrmàn ansatz to magnetohydrodynamics. Meccanica 21:81–86
23. Andersson HI, de Korte E (2002) MHD flow of a power-law fluid over a rotating disk. Eur J Mech B-Fluids 21:317–324
24. Takhar HS, Singh AK, Nath G (2002) Unsteady mhd flow and heat transfer on a rotating disk in an ambient fluid. Int J Therm Sci 41:147–155
25. Hayat T, Hameed MI, Asghar S, Siddiqui AM (2004) Some steady MHD flows of the second order fluid. Meccanica 39:345–355
26. Hilton PJ (1953) An introduction to homotopy theory. Cambridge University Press

27. Sen S (1983) Topology and geometry for physicists. Academic Press, Florida
28. Liao SJ (1992) The proposed homotopy analysis techniques for the solution of nonlinear problems. Ph.D. dissertation (in English), Shanghai Jiao Tong University, Shanghai
29. Liao SJ (1992) A second-order approximate analytical solution of a simple pendulum by the Process Analysis method. J Appl Mech-Trans ASME 59:970–975
30. Liao SJ (1995) A kind of approximate solution technique which does not depend upon small parameters: a special example. Int J Non-Linear Mech 30:371–380
31. Liao SJ (1997) A kind of approximate solution technique which does not depend upon small parameters (II): an application in fluid mechanics. Int J Non-Linear Mech 32:815–822
32. Liao SJ (1999) An explicit, totally analytic approximation of Blasius viscous flow problems. Int J Non-Linear Mech 34:759–778
33. Liao SJ (2004) On the homotopy analysis method for nonlinear problems. Appl Math Comput 147:499–513
34. Lyapunov AM (1892) General problem on stability of motion (English translation). Taylor & Francis, London, 1992
35. Adomian G (1976) Nonlinear stochastic differential equations. J Math Anal Appl 55:441–452
36. Karmishin AV, Zhukov AT, Kolosov VG (1990) Methods of dynamics calculation and testing for thin-walled structures (in Russian). Mashinostroyenie, Moscow
37. Liao SJ (2003) Beyond Perturbation: Introduction to Homotopy Analysis Method. Chapman & Hall/ CRC Press, Boca Raton
38. He JH (1999) Homotopy perturbation technique. Comput Methods Appl Mech Eng 178:257–262
39. Liao SJ (2005) Comparison between the homotopy analysis method and homotopy perturbation method. Appl Math Comput 169:1186–1194
40. Liao SJ (1999) A uniformly valid analytic solution of two-dimensional viscous flow over a semi-infinite flat plate. J Fluid Mech 385:101–128
41. Liao SJ (2002) An analytic approximation of the drag coefficient for the viscous flow past a sphere. Int J Nonlinear Mech 37:1–18
42. Liao SJ, Campo A (2002) Analytic solutions of the temperature distribution in Blasius viscous flow problems. J Fluid Mech 453:411–425
43. Li SC, Liao SJ (2005) An analytic approach to solve multiple solutions of a strongly nonlinear problem. Appl Math Comput 169:854–865
44. Xu H (2005) An explicit analytic solution for convective heat transfer in an electrically conducting fluid at a stretching surface with uniform free stream. Int J Eng Sci 43:859–874
45. Liao SJ (2006) An analytic solution of unsteady boundary-layer flows caused by an impulsively stretching plate. Commun Nonlinear Sci Num Simulat 11:326–339
46. Xu H, Liao SJ (2005) Series solutions of unsteady magnetohydrodynamic flows of non-Newtonian fluids caused by an impulsively stretching plate. J Non-Newton Fluid Mech 159:46–55
47. Cheng J, Liao SJ, Pop I (2005) Analytic series solution for unsteady mixed convection boundary layer flow near the stagnation point on a vertical surface in a porous medium. Transport Porous Media 61:365–379
48. Liao SJ (2005) A new branch of solutions of boundary-layer flows over a permeable stretching plate. Int J Heat Mass Transfer 48:2529–2539
49. Liao SJ, Magyari E (in press) Exponentially decaying boundary layers as limiting cases of families of algebraically decaying ones. ZAMP
50. Eringen AC, Maugin GA (1990) Electrodynamics of continua, vol 2. Springer, Berlin
51. Williams JC, Rhyne TH (1980) Boundary layer development on a wedge impulsively set into motion. SIAM J Appl Math 38:215–224
52. Cebeci T, Bradshaw P (1988) Physical and computational aspects of convective heat transfer. Springer, New York